



**Dispersion Forces Play a Role in (Me<sub>2</sub>IPr)Fe(=NAd)R<sub>2</sub> (Ad = adamantyl; R = neoPe, 1-nor) Insertions and Fe-R Bond Dissociation Enthalpies**

Journal:	<i>Dalton Transactions</i>
Manuscript ID	DT-ART-11-2017-004145.R2
Article Type:	Paper
Date Submitted by the Author:	11-Apr-2018
Complete List of Authors:	Cundari, Thomas; University of North Texas, Chemistry Jacobs, Brian; Cornell University, Dept. of Chemistry & Chemical Biology MacMillan, Samantha; Cornell University, Chemistry and Chemical Biology Wolczanski, Peter; Cornell University, Dept. of Chemistry & Chemical Biology



Journal Name

ARTICLE

## Dispersion Forces Play a Role in $(\text{Me}_2\text{IPr})\text{Fe}(=\text{NAd})\text{R}_2$ (Ad = adamantyl; R = <sup>neo</sup>Pe, 1-nor) Insertions and Fe-R Bond Dissociation Enthalpies

Received 00th January 20xx,  
Accepted 00th January 20xx

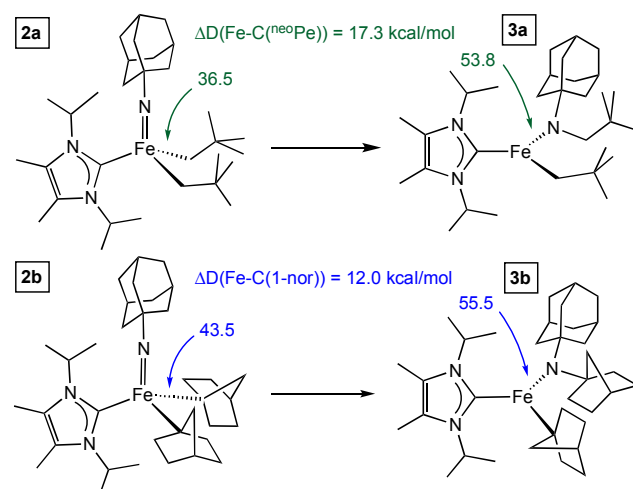
Thomas R. Cundari\*,<sup>a</sup> Brian P. Jacobs,<sup>b</sup> Samantha N. MacMillan,<sup>b</sup> and Peter T. Wolczanski\*<sup>b</sup>

DOI: 10.1039/x0xx00000x

www.rsc.org/

### Table of Contents Graphic

Calculations show that dispersion forces in four-coordinate  $(\text{Me}_2\text{IPr})\text{Fe}(=\text{NAd})(1\text{-nor})_2$  (**2b**) contribute to greater  $D(\text{FeR})$  and slow its migratory insertion relative to the neopentyl analogue.



<sup>a</sup> Department of Chemistry, CASCaM, University of North Texas, Denton, Texas 76201, USA.

<sup>b</sup> Department of Chemistry and Chemical Biology, Baker Laboratory, Cornell University, Ithaca, NY 14853, USA.

† e-mail: ptw2@cornell.edu; Thomas.Cundari@unt.edu

Electronic Supplementary Information (ESI) available: experimental and calculational details, and spectroscopic information. See DOI: 10.1039/x0xx00000x



Journal Name

ARTICLE

## Dispersion Forces Play a Role in (Me<sub>2</sub>IPr)Fe(=NAd)R<sub>2</sub> (Ad = adamantyl; R = <sup>neo</sup>Pe, 1-nor) Insertions and Fe-R Bond Dissociation Enthalpies (BDEs)

Thomas R. Cundari\*,<sup>a</sup> Brian P. Jacobs,<sup>b</sup> Samantha N. MacMillan,<sup>b</sup> and Peter T. Wolczanski\*<sup>b</sup>

Received 00th January 20xx,  
Accepted 00th January 20xx

DOI: 10.1039/x0xx00000x

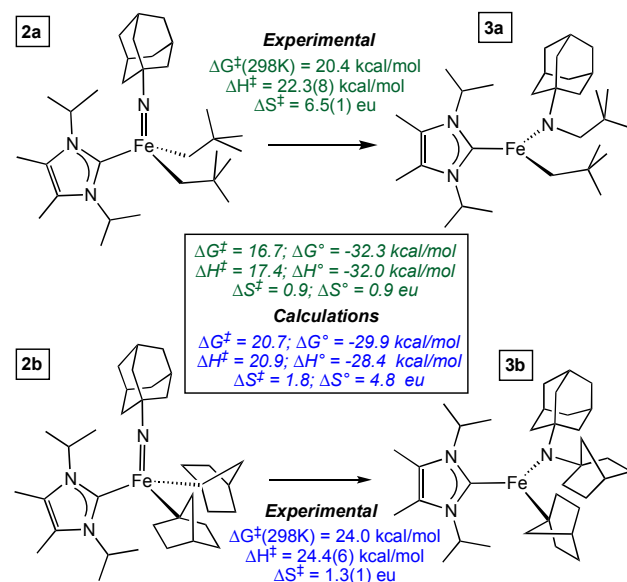
www.rsc.org/

The effects of dispersion on migratory insertion reactions and related iron-carbon bond dissociation energies pertaining to (Me<sub>2</sub>IPr)FeR<sub>2</sub> (R = <sup>neo</sup>Pe, 1-nor), and the conversion of (Me<sub>2</sub>IPr)Fe(=NAd)R<sub>2</sub> to (Me<sub>2</sub>IPr)Fe(N(Ad)R)R are investigated via calculations and structural comparisons. Dispersion appears to be an underappreciated, major contributor to common structure and reactivity relationships.

### Introduction

Dedicated to Philip P. Power, synthetic chemist extraordinaire, on the occasion of his 65th birthday

In a recent communication,<sup>1</sup> the relative rates of a rare imide insertion into a metal-carbon bond was reported. The process, which is shown in Scheme 1, is the conversion of an intermediate



**Scheme 1.** Experimental and calculated activation parameters for imide insertions, and calculated  $\Delta G^\circ$ ,  $\Delta H^\circ$  and  $\Delta S^\circ$ .

spin ( $S = 1$ ), formally iron(IV) (Me<sub>2</sub>IPr)Fe(=NAd)R<sub>2</sub> (Ad = adamantyl; R

= <sup>neo</sup>Pe (2a), 1-nor (2b)), generated from the corresponding dialkyls (1a,b) and adamantyl azide, to a high spin ( $S = 2$ ) iron(II) amide-alkyl, (Me<sub>2</sub>IPr)Fe(N(Ad)R)R (R = <sup>neo</sup>Pe (3a), 1-nor (3b)). Calculations supporting the mechanism proved less than satisfactory unless dispersion corrections were incorporated.

Power et al.<sup>2</sup> have suggested that dispersion is a crucial stabilization factor in congested, and low coordinate transition metal compounds.<sup>3</sup> For example, dispersion forces are thought to provide favorable interligand energies in M(1-nor)<sub>4</sub> (M = Fe, 45.9 kcal/mol; Co, 38.3 kcal/mol)<sup>2</sup> as inferred from calculations of 1-nor homolysis. Fürstner has attributed the modest stability of Fe(<sup>c</sup>Hex)<sub>4</sub><sup>4</sup> in part to similar forces. As a consequence, it is worth investigating the importance of dispersion<sup>5-7</sup> in bond homolysis, and related contributions to other unimolecular processes,<sup>8,9</sup> such as migratory insertion.

In assessing the insertion reactions illustrated in Scheme 1 via calculations, the more favorable enthalpy of converting **2a**→**3a** ( $\Delta H^\circ = -32.0 \text{ kcal/mol}$ ) vs. **2b**→**3b** ( $-29.9 \text{ kcal/mol}$ ) translates into a lower barrier (17.4 vs. 20.9 kcal/mol). What is the origin of the greater driving force that leads to faster rates for R= neopentyl vs. R = 1-norbornyl?

Calculations (Table 1) on the homolysis of the iron-alkyl bonds suggested that the difference between the Fe(IV)-R and Fe(II)-R species were significantly greater for R = <sup>neo</sup>Pe ( $\Delta\Delta H^\circ = -17.3 \text{ kcal/mol}$ ) vs. R = 1-nor ( $\Delta\Delta H^\circ = -12.0 \text{ kcal/mol}$ ). Note that the primary difference was in the Fe(IV) species, **2a** vs. **2b**, where the 1-norbornyl derivative was calculated to have a 7.0 kcal/mol greater bond dissociation enthalpy (BDE), whereas it was only calculated to be 1.7 kcal/mol stronger in the ferrous product, **3a** vs. **3b**. Herein it is suggested that dispersion plays a significant role in the BDE disparity, and other structural comparisons support the importance of dispersion.

<sup>a</sup> Department of Chemistry, CASCaM, University of North Texas, Denton, Texas 76201, USA.

<sup>b</sup> Department of Chemistry and Chemical Biology, Baker Laboratory, Cornell University, Ithaca, NY 14853, USA.

† e-mail: ptw2@cornell.edu; Thomas.Cundari@unt.edu

Electronic Supplementary Information (ESI) available: experimental and calculational details, and spectroscopic information. See DOI: 10.1039/x0xx00000x

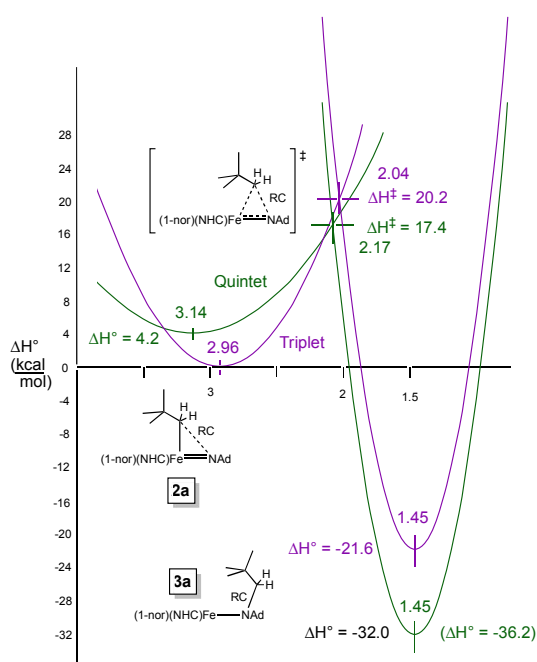
**Table 1.** Calculated (with and without dispersion) ground state BDEs and BDFEs for the homolytic dissociation of R ([Fe] = (Me<sub>2</sub>IPr)Fe) in kcal/mol.

iron alkyl species	BDE <sup>a</sup>		$\Delta^c$	BDFE <sup>d</sup>		$\Delta^c$
	(w)	(w/o)		(w)	(w/o)	
[Fe] <sup>(neo)Pe</sup> <sub>2</sub> ( <b>1a</b> )	51.1	34.8	16.3	35.5	21.7	13.8
[Fe](1-nor) <sub>2</sub> ( <b>1b</b> )	57.0	36.0	21.0	42.2	24.0	18.2
[Fe](=NAd) <sup>(neo)Pe</sup> <sub>2</sub> ( <b>2a</b> , S = 1)	36.5 <sup>d</sup>	13.6 <sup>d</sup>	22.9 <sup>d</sup>	18.1 <sup>d</sup>	-4.1 <sup>d</sup>	22.2 <sup>d</sup>
( <b>2a</b> , S = 3)	32.3 <sup>e</sup>	11.4 <sup>e</sup>	20.9 <sup>e</sup>	15.2 <sup>e</sup>	-4.5 <sup>e</sup>	19.7 <sup>e</sup>
[Fe](=NAd)(1-nor) <sub>2</sub> ( <b>2b</b> , S = 1)	43.5 <sup>d</sup>	16.7 <sup>d</sup>	26.8 <sup>d</sup>	26.0 <sup>d</sup>	-0.8 <sup>d</sup>	26.8 <sup>d</sup>
( <b>2b</b> , S = 3)	39.5 <sup>e</sup>	15.6 <sup>e</sup>	23.9 <sup>e</sup>	24.0 <sup>d</sup>	-0.2 <sup>e</sup>	24.2 <sup>e</sup>
[Fe]{N(Ad) <sup>(neo)Pe</sup> } <sub>2</sub> ( <b>3a</b> )	53.8	37.0	16.8	36.2	22.0	14.2
[Fe]{N(Ad)(1-nor)} <sub>2</sub> ( <b>3b</b> )	55.5	35.5	20.0	41.2	21.8	19.4
[Fe]{N(NCPh <sub>2</sub> )(1-nor)} <sub>2</sub> ( <b>4b</b> )	49.6	29.9	19.7	34.5	16.5	18.0

<b>2a</b> (S = 1) → <b>3a</b> (S = 1) <sup>f</sup>	-17.3 <sup>d</sup>	-23.4 <sup>d</sup>	-18.1 <sup>d</sup>	-26.1 <sup>d</sup>
	-21.5 <sup>e</sup>	-25.6 <sup>e</sup>	-21.0 <sup>e</sup>	-26.5 <sup>e</sup>
<b>2b</b> (S = 1) → <b>3b</b> (S = 1) <sup>f</sup>	-12.0 <sup>d</sup>	-18.8 <sup>d</sup>	-15.2 <sup>d</sup>	-22.6 <sup>d</sup>
	-16.0 <sup>e</sup>	-19.9 <sup>e</sup>	-17.2 <sup>e</sup>	-22.0 <sup>e</sup>

<sup>a</sup>B3PW91-GD3/G-31+G(d) w/dispersion. <sup>b</sup>B3PW91/G-31+G(d) without dispersion. <sup>c</sup> $\Delta = \Delta\text{BDE} = \text{BDE}(w/\text{disp}) - \text{BDE}$ ;  $\Delta = \Delta\text{BDFE} = \text{BDFE}(w/\text{disp}) - \text{BDFE}$ . <sup>d</sup>Triplet GS. <sup>e</sup>Quintet excited state (ES, *italicized*). <sup>f</sup> $\Delta\Delta\text{H}$  and  $\Delta\Delta\text{G}$  values for the conversion described.



**Figure 1.** Parabolic fit of metric parameters and enthalpies pertaining to the insertion reaction: (Me<sub>2</sub>IPr)Fe(=NAd)<sup>(neo)Pe</sup><sub>2</sub> (**2a**) → (Me<sub>2</sub>IPr)Fe{N(Ad)<sup>(neo)Pe</sup>}<sub>2</sub> (**3a**); x-axis is d(NC) = RC as per dashed lines.

## Results and discussion

### Reaction Coordinates

Prior to assessing factors that address BDEs, it is important to determine whether a simple insertion reaction coordinate (RC) that has substantial iron-carbon bond breaking is reasonable. Using

metric parameters and energies of the ground states (GSs) and transition states (TSs) supplied by the calculations, a RC consisting of the N(imide) to alkyl distance was explored. Fig. 1 illustrates the (Me<sub>2</sub>IPr)Fe(=NAd)<sup>(neo)Pe</sup><sub>2</sub> (**2a**) insertion process to afford (Me<sub>2</sub>IPr)Fe{N(Ad)<sup>(neo)Pe</sup>}<sub>2</sub> (**3a**), using parabolic enthalpy surfaces. Intersystem crossing from the GS triplet of **2a** to its corresponding quintet surface, *prior* to the transition state of insertion, is in accord with the calculation of a lower lying quintet TS.<sup>1</sup> As a consequence, a straightforward RC of Fe-C(<sup>neo</sup>Pe) bond-breaking and N-C(<sup>neo</sup>Pe) bond making is deemed reasonable. The transition state is characterized by an imaginary frequency at 303 cm<sup>-1</sup>.

Fig. 2 illustrates the related parabolic diagram pertaining to the insertion of the 1-norbornyl derivative: (Me<sub>2</sub>IPr)Fe(=NAd)(1-nor)<sub>2</sub> (**2b**) → (Me<sub>2</sub>IPr)Fe{N(Ad)(1-nor)}<sub>2</sub> (**3b**). Once again, the migratory insertion path faithfully reproduces an intersystem crossing event from the triplet to quintet **2b** surfaces that occurs before the transition state.<sup>1</sup> The 285 cm<sup>-1</sup> imaginary frequency that characterizes the TS is consistent with its higher energy with respect to that of the <sup>neo</sup>Pe case. It is likely that the quintet TS of the **2a**→**3a** system has greater triplet character due to its closer energy to the intersystem crossing event. Greater mixing in this <sup>neo</sup>Pe case can also contribute to the higher frequency relative to the 1-nor system.

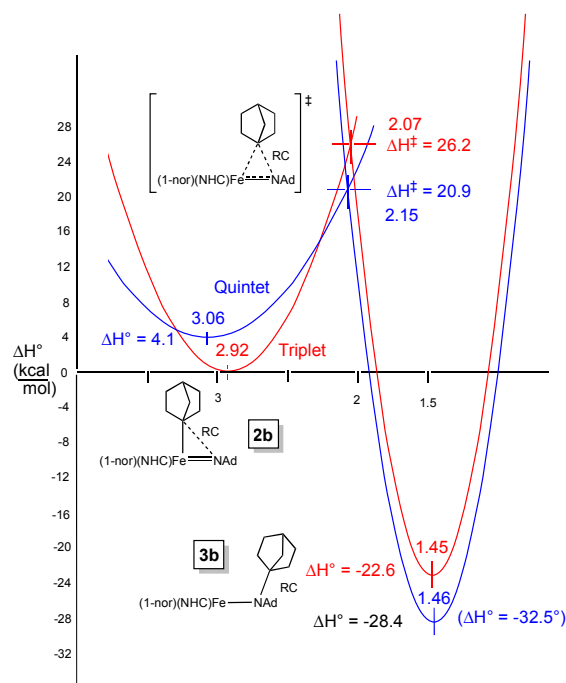


**Figure 2.** Parabolic fit of metric parameters and enthalpies pertaining to the insertion reaction: (Me<sub>2</sub>IPr)Fe(=NAd)(1-nor)<sub>2</sub> (**2b**) → (Me<sub>2</sub>IPr)Fe{N(Ad)(1-nor)}<sub>2</sub> (**3b**); x-axis is d(NC) = RC as per dashed lines.

### Factors influencing insertion rates via BDEs

Now that the reaction coordinate has been explored and is shown to be consistent with elements of Fe-C bond breaking, factors that influence the BDEs of the two systems can be analyzed. Experimental carbon-hydrogen bond energies for <sup>neo</sup>Pe-H and (1-nor)H are 100.3 (99.4 (calc)) and 96.7 (104.2 calc; 105.5 (G4 *ab initio*)) kcal/mol, respectively.<sup>10</sup> The (1-nor)H BDE is somewhat higher than expected (e.g., Me<sub>3</sub>CH, BDE = 95.7 kcal/mol, 92.1 calc,

96.0 (G4 *ab initio*) due to the "tied-back" nature of the tertiary carbon on norbornane, which imparts slightly more *s*-character (26% vs 22% in isobutane) to the bridgehead position. The experimental C-H BDEs suggest that corresponding Fe-C(<sup>neo</sup>Pe) bonds should be stronger than the Fe-C(1-nor) interactions,<sup>11-13</sup> but *calculations do not support this statement*.

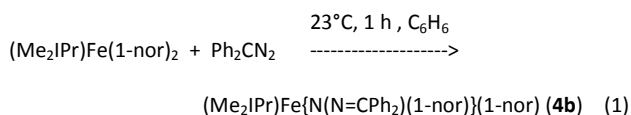
A perusal of the calculated BDEs and BDFEs (bond dissociation free energies) in Table 1 shows that the 1-norbornyl derivatives are greater than the neopentyl cases in all three compound types: (Me<sub>2</sub>IPr)FeR<sub>2</sub> (**1**), (Me<sub>2</sub>IPr)Fe(=NAd)R<sub>2</sub> (**2**), and (Me<sub>2</sub>IPr)Fe(N(Ad)(R))R (**3**). More importantly, dispersion contributes a substantial amount to the stabilization of all of these complexes. For example, the BDEs (without dispersion) for the Fe(IV) (**2**) species indicate that the complexes would be unstable if not for contributions due to dispersion.

The aforementioned linear free energy relationship that is believed responsible for the faster rate of **2a**→**3a** vs. **2b**→**3b** originates in the calculated BDE difference (5.3 kcal/mol) between the Fe(IV)-R and Fe(II)-R species: R = <sup>neo</sup>Pe, ΔΔH° = -17.3 kcal/mol; R = 1-nor, ΔΔH° = -12.0 kcal/mol. When dispersion is removed from the calculations, the neopentyl case is still favored by slightly less (4.6 kcal/mol). Differences in dispersion factors are slightly greater between the Fe(IV) derivatives, where the iron-carbon bond strengths are 7.0 kcal/mol stronger for **2b** vs. **2a**; they are only 1.7 stronger for **3b** vs. **3a**. BDE calculations without dispersion show only a 3.1 kcal/mol difference, and the D(FeC) in **3a** is actually 1.5 kcal/mol stronger than in **3b**. Given these results, it is also quite plausible that the experimental BDEs on (1-nor)H are not viable.

In summary, dispersion forces account for 31-37% of the BDE for the three-coordinate (Me<sub>2</sub>IPr)FeR<sub>2</sub> (**1**) and (Me<sub>2</sub>IPr)Fe(N(Ad)(R))R (**3**) species, and 62-63% of the BDE in the more sterically congested four coordinate imido complexes, (Me<sub>2</sub>IPr)Fe(=NAd)R<sub>2</sub> (**2**). The influence of dispersion is greater for the 1-norbornyl complexes, and the slower rate of insertion for the 1-nor case (**2b**→**3b**) vs. the <sup>neo</sup>Pe system is subtly impacted by this difference.

#### (Me<sub>2</sub>IPr)Fe{N(N=CPh<sub>2</sub>)}(1-nor){1-nor}: Synthesis, Structure and Calculation

Common to both insertion processes is the adamantyl group attached to the imide in (Me<sub>2</sub>IPr)Fe(=NAd)R<sub>2</sub> (R = <sup>neo</sup>Pe (**2a**), 1-nor (**2b**)), and the amide in (Me<sub>2</sub>IPr)Fe{N(Ad)R}R (R = <sup>neo</sup>Pe (**3a**), 1-nor (**3b**)). While no other Fe(IV) imides proved stable enough to provide an experimental comparison, treatment of (Me<sub>2</sub>IPr)Fe(1-nor)<sub>2</sub> with Ph<sub>2</sub>CN<sub>2</sub><sup>14-17</sup> did provide another Fe(II) amide complex, (Me<sub>2</sub>IPr)Fe{N(N=CPh<sub>2</sub>)}(1-nor) (**4b**, 57%), according to eq 1. No



intermediates were detected, as the solution merely darkened from light-yellow to orange-brown, consistent with transient imide formation and rapid insertion. The μ<sub>eff</sub>, conducted via Evans' method,<sup>18</sup> was 4.7 μ<sub>B</sub>, consistent with an *S* = 2 center.

Fig. 3 illustrates a molecular view of (Me<sub>2</sub>IPr)Fe{N(N=CPh<sub>2</sub>)}(1-nor) (**4b**), replete with pertinent bond distances and angles. The complex is pseudo trigonal, although the core angles only sum to 355.28°, as the iron is slightly out of the plane, and directed toward a phenyl group, with long Fe-C<sub>ortho</sub> and Fe-H(C<sub>ortho</sub>) contact

distances of 2.65 and 2.74 Å. The Fe-C(NHC) and Fe-C(Ad) bond distances are 2.1450(16) and 2.0780 Å, respectively, and the iron-nitrogen distance of 2.0023(14) Å is consistent with a single bond of an amide. Additional metric parameters of the amide linkage support the Fe-N(1-nor)-N=CPh<sub>2</sub> formulation.

Calculations of the iron-1-norbornyl bond dissociation energy and free energy pertaining to (Me<sub>2</sub>IPr)Fe{N(N=CPh<sub>2</sub>)}(1-nor) (**4b**) afford slightly smaller values than that of (Me<sub>2</sub>IPr)Fe{N(Ad)}(1-nor) (**3b**). Differences in BDE calculated with and without dispersion (ΔBDE = 19.7 kcal/mol) are essentially the same as in **3b**. The system has other components that do not permit a ready comparison of adamantyl vs. Ph<sub>2</sub>C=N group effects, especially since the likely imide precursor was not observed.

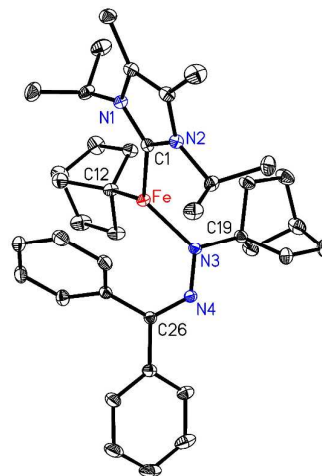
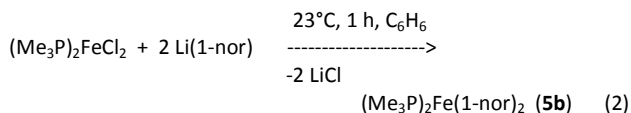


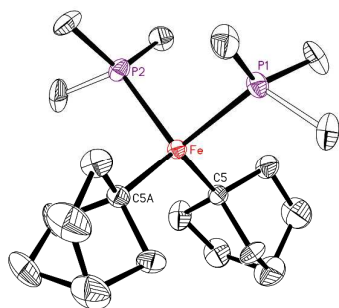
**Figure 3.** Molecular view of (Me<sub>2</sub>IPr)Fe{N(N=CPh<sub>2</sub>)}(1-nor)(1-nor) (**4b**). Interatomic distances (Å) and angles (°): Fe-N3, 2.0023(14); Fe-C1, 2.1450(16); Fe-C12, 2.0780(17); N3-N4, 1.3521(18); N4-C26, 1.305(2); N3-C19, 1.457(2); N3-Fe-C12, 113.41(6); N3-Fe-C1, 117.91(6); C1-Fe-C12, 123.96(6); Fe-N3-N4, 128.29(10); Fe-N3-C19, 119.90(10); N3-N4-C26, 121.57(14).

#### (Me<sub>3</sub>P)Fe(1-nor)<sub>2</sub>: Synthesis, Structure and Isodesmic Calculation

In Power's initial study of the impact of dispersion on Fe(1-nor)<sub>2</sub>,<sup>2</sup> an isodesmic calculation was used to show the effect on an equilibrium with "FeH<sub>4</sub>". In order to corroborate these findings, and those of the preceding 1-norbornyl derivatives, a related isodesmic reaction was calculated. First, treatment of (Me<sub>3</sub>P)<sub>2</sub>FeCl<sub>2</sub><sup>19</sup> with 2 equiv of (1-nor)Li produced off-white (Me<sub>3</sub>P)<sub>2</sub>Fe(1-nor)<sub>2</sub> (**5b**) in 61% yield.

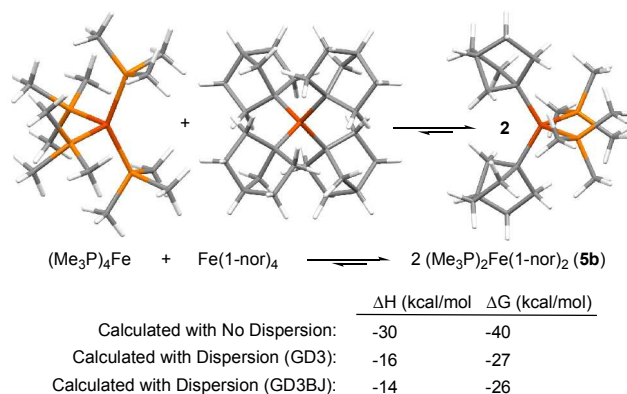


Evans' method<sup>18</sup> measurements of **5b** gave a μ<sub>eff</sub> of 4.7 μ<sub>B</sub>, consistent with a pseudo tetrahedral *S* = 2 system.



**Figure 4.** Molecular view of highly disordered  $(\text{Me}_3\text{P})_2\text{Fe}(\text{1-nor})_2$  (**5b**). Interatomic distances (Å) and angles ( $^\circ$ ): Fe-C5, 2.057(2); Fe-P1, 2.4127(10); Fe-P2, 2.4076(9); C5-Fe-C5A, 120.32(12); C5(C5A)-Fe-P2, 108.50(7); C5(C5A)-Fe-P1, 109.00(6); P1-Fe-P2, 99.53(4).

Despite severe rotational disorders in the 1-norbornyl and  $\text{PMe}_3$  ligands, a reasonable structural model for  $(\text{Me}_3\text{P})_2\text{Fe}(\text{1-nor})_2$  (**5b**) was obtained via X-ray crystallography, and a molecular view is illustrated in Fig. 4. The C-Fe-C angle pertaining to the 1-nor groups is  $120.32(12)^\circ$ , while the phosphorus atoms are  $99.53(4)^\circ$  apart, and all remaining core angles are  $108.75(29)^\circ$ . The bond distances of 2.057(2) and 2.410(4) Å pertaining to  $d(\text{Fe-C})$  and  $d(\text{Fe-P})$ , respectively, are normal for tetrahedral ferrous species.



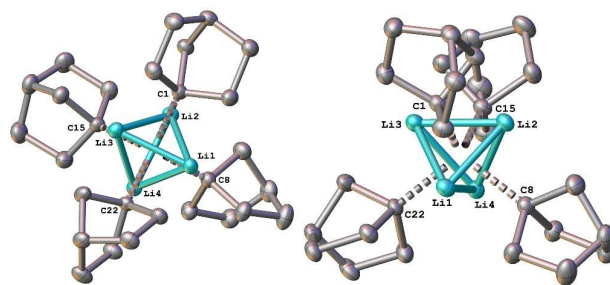
**Figure 5.** Calculated  $\Delta H$  and  $\Delta G$  for the comproportionation of  $(\text{Me}_3\text{P})_4\text{Fe} + \text{Fe}(\text{1-nor})_4$  to  $2 (\text{Me}_3\text{P})_2\text{Fe}(\text{1-nor})_2$  (**5b**) with and without corrections due to dispersion.

Fig. 5 shows the isodesmic reaction of  $\text{Fe}(\text{1-nor})_4$  and  $(\text{Me}_3\text{P})_4\text{Fe}$  comproportionating to two equiv of  $(\text{Me}_3\text{P})_2\text{Fe}(\text{1-nor})_2$  (**5b**). First, note that  $(\text{Me}_3\text{P})_4\text{Fe}$  actually exists as  $(\text{Me}_3\text{P})_3\text{HFe}(\eta^2\text{-CH}_2\text{PMe}_2)$ ,<sup>20</sup> but its reactivity is akin to the iron(0) tetrakis-phosphine species, and is thus considered close in energy. Depending on the levels of theory utilized, dispersion accounts for  $\sim 15$  kcal/mol of enthalpic stabilization in the homoleptic complexes, mostly in  $\text{Fe}(\text{1-nor})_4$ . The six (1-nor)/(1-nor) interactions on the reactant side are offset by two in the products, one for each **5b**. While the magnitude per 1-nor ligand is less than claimed for  $\text{Fe}(\text{1-nor})_4$  alone,<sup>2</sup> these results – all on known, isolable (or isomeric in the case of  $(\text{Me}_3\text{P})_4\text{Fe}$ ) complexes – support the contention that dispersion plays a crucial role in low coordinate complexation. The lower values are undoubtedly due to the fact that dispersion via the  $\text{PMe}_3$  ligands contributes substantially, albeit at longer distances due to the  $d(\text{Fe-P})$  being  $\sim 0.35$  Å longer than the  $d(\text{Fe-C})$ .

Note that the comproportionation of Fe(0) and Fe(IV) to two equiv Fe(II) is favorable in the isodesmic calculation above, in contrast to the synthesis of  $\text{Fe}(\text{1-nor})_4$ ,<sup>21,22</sup> which is prepared from (1-nor)Li and Fe(II) sources in weakly donating solvents. Theopold's related studies on  $[\text{Co}(\text{1-nor})_4]^n$  ( $n = -1, 0, +1$ )<sup>23</sup> helped show that disproportionation to M(IV) and M(0) is the likely path for iron and cobalt. The maximization of dispersion is a plausible factor enabling formation of the M(IV) species, but if a significant donor ligand is also present, as in the  $\text{PMe}_3$  case above, iron(II) persists as the stable form. Presumably, favoring Fe(II)<sup>24</sup> entails both ligand donor interactions as well as, at least in the case of  $\text{PMe}_3$ , additional dispersion factors.

#### [(1-nor)Li]<sub>4</sub>: Structure and Isodesmic Calculation

The use of the 1-nor group to stabilize tetrahedral M(1-nor)<sub>4</sub> transition metal complexes, and its high degree of covalence in the corresponding high formal oxidation state metal-carbon bonds, prompted a structural study of Li(1-nor) aggregates.



**Figure 6.** Two molecular views of tetrameric  $[(\text{1-nor})\text{Li}]_4$ . Interatomic distances (Å) and angles ( $^\circ$ ): Li1-C1, 2.213(5); Li-C8, 2.190(5); Li1-C22, 2.219(5); Li2-C1, 2.225(5); Li2-C8, 2.217(5); Li2-C15, 2.190(5); Li3-C1, 2.193(5); Li3-C15, 2.230(5); Li3-C22, 2.217(5); Li4-C8, 2.190(5); Li4-C15, 2.198(5); Li4-C22, 2.189(5); Li-Li, 2.419(17) (ave).

Crystallization of  $(\text{1-nor})\text{Li}$ <sup>23,25</sup> from pentane solvent afforded a tetramer, whose structure is illustrated in Fig. 6. The lithium atoms are disposed in a regular tetrahedron, with  $d(\text{Li-Li}) = 2.419(17)$  Å (ave). The  $\alpha$ -carbons of each 1-norbornyl unit are equidistant to each  $\text{Li}_3$  face, with  $d(\text{C}(\alpha)\text{-Li}) = 2.206(16)$  Å (ave). Interactions of the  $\beta$ -carbons with the lithium atoms range from 2.3 to 3.6 Å.

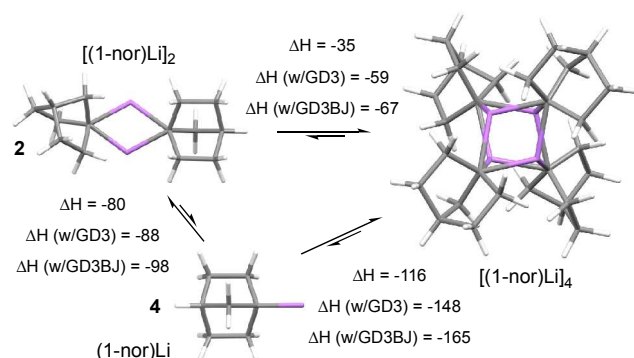


**Figure 7.**  $\Delta H$  (kcal/mol) for tetramerization and dimerization of (1-nor)Li and [(1-nor)Li]<sub>2</sub> to [(1-nor)Li]<sub>4</sub>, calculated without and with (GD3, GD3BJ) dispersion.

Fig.7 depicts the gas phase dimerization of [(1-nor)Li]<sub>2</sub> and tetramerization of (1-nor)Li to tetrahedral [(1-nor)Li]<sub>4</sub> with associated enthalpies calculated with and without empirical dispersion. Assuming six (1-nor)/(1-nor) interactions in the tetramer, dispersion accounts for ~30-40 kcal/mol, or roughly 6-8 kcal/mol per interaction relative to 4 (1-nor)Li. The amount of dispersive energy in each aggregation is method dependent with the GD3BJ correction giving the higher values.

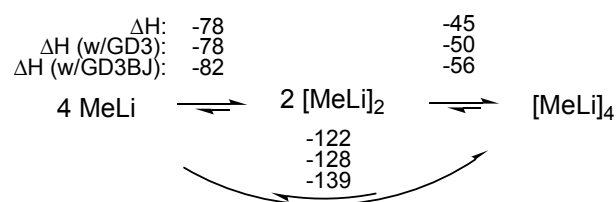


**Figure 8.**  $\Delta H$  (in kcal/mol) for tetramerization and dimerization of MeLi and [MeLi]<sub>2</sub> to [MeLi]<sub>4</sub>, calculated without and with (GD3, GD3BJ) dispersion.

Since the bonding of each RLi fragment differs in the monomer and each aggregate, it is imperative to compare the [(1-nor)Li]<sub>n</sub> systems with one in which a significantly smaller amount of dispersion is likely. Fig. 8 illustrates the related case of MeLi aggregation, which manifests similar enthalpic changes, but less correction from dispersion. Even for the tetramerization of MeLi, dispersion contributes 6-17 kcal/mol, whereas the corresponding tetramerization of (1-nor)Li has a corresponding 32-49 kcal/mol. It is noteworthy that such corrections appear important even for small RLi.

## Conclusions

According to the calculations herein, there is no question that dispersion is consequential to structural stability. As an enthalpic contribution, chemical reactivity and affiliated rates can also be affected. The magnitude of these effects is surprising, especially the realization that simple bond dissociation enthalpies can have a substantial dispersion component.

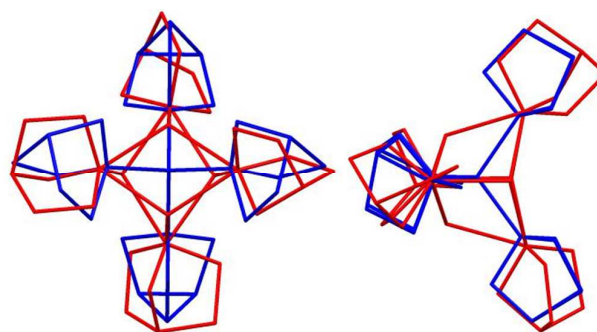


**Figure 9.** Wireframe views of the superposition of Fe(1-nor)<sub>4</sub> (blue) and [(1-nor)Li]<sub>4</sub>, clearly showing structurally related 1-norbornyl groups, which likely lead to similar dispersion interactions.

The results above, prompted by the observations of Power et al.,<sup>2-4</sup> show that the forces of dispersion have been underappreciated in areas outside of solvation and materials.<sup>26,27</sup> Consider the structures of Fe(1-nor)<sub>4</sub> and [(1-nor)Li]<sub>4</sub> illustrated in Fig. 9. It appears reasonable that the same force is critical in holding these disparate species to their tetrahedral geometries, and that force is likely to be dispersion.

This work also serves to highlight dispersion as a force that needs to be considered in systems featuring large hydrocarbons. It must be emphasized that the magnitudes of dispersion factors, while a point of emphasis in this research, should be appreciated as method dependent. The model used herein was introduced by Powers, Nagase, and coworkers,<sup>2,9</sup> and was chosen for comparison. It is also important to recognize that gas phase calculations are utilized herein, and solvation dispersion forces, say in stabilizing the fragments of homolytic bond dissociation, may impact interpretations. Recent evidence supports the contention that ligand/substrate dispersion interactions play crucial roles in catalytic selectivities.<sup>28</sup>

## Conflicts of interest

There are no conflicts to declare.

## Acknowledgements

We gratefully acknowledge financial support of the NSF (PTW: CHE-1664580; Cornell NMR Facility, CHE-1531632. TRC: CHE-1531468 (CASCAM)), and the DOE (TRC: DE-FG02-03ER15387).

## Notes and references

Complexes **1a,b**, **2a,b**, **3a,b**,<sup>1</sup> and [(1-nor)Li]<sub>4</sub><sup>22,23</sup> were prepared via literature methods. Amide **4b** and dialkyl **5b** were prepared as described in the text. For full experimental and calculational details, see the supplementary information.

*Crystal data for 4b:* C<sub>38</sub>H<sub>52</sub>N<sub>4</sub>Fe, *M* = 620.68, monoclinic, P2<sub>1</sub>/c, *a* = 10.4328(4), *b* = 20.1032(7), *c* = 17.3563(6) Å, β = 106.003(2)°, *V* = 3499.1(2) Å<sup>3</sup>, *T* = 223(2) K, λ = 0.71073 Å, *Z* = 4, *R*<sub>int</sub> = 0.0408, 37447 reflections, 8039 independent, *R*<sub>1</sub>(all data) = 0.0589, *wR*<sub>2</sub> = 0.0949, *GOF* = 1.012, CCDC-1583545.

*Crystal data for 5b*: C<sub>20</sub>H<sub>40</sub>P<sub>2</sub>Fe, *M* = 398.31, orthorhombic, Pnma, *a* = 18.2193(12), *b* = 14.0581(7), *c* = 9.3097(6) Å, *V* = 2384.5(2) Å<sup>3</sup>, *T* = 223(2) K,  $\lambda$  = 0.71073 Å, *Z* = 4, *R*<sub>int</sub> = 0.0285, 20682 reflections, 2271 independent, *R*<sub>1</sub>(all data) = 0.0467, *wR*<sub>2</sub> = 0.1282, GOF = 1.082, CCDC-1583546.

*Crystal data for [(1-nor)Li]<sub>4</sub>*: C<sub>28</sub>H<sub>44</sub>Li<sub>4</sub>, *M* = 408.39, monoclinic, P2<sub>1</sub>, *a* = 10.3771(2), *b* = 10.1982(2), *c* = 11.7698(2) Å, *V* = 1245.57(4) Å<sup>3</sup>, *T* = 100.0(10) K,  $\lambda$  = 0.71073 Å, *Z* = 2, *R*<sub>int</sub> = 0.0410, 33926 reflections, 5229 independent, *R*<sub>1</sub>(all data) = 0.0428, *wR*<sub>2</sub> = 0.1123, GOF = 1.069, CCDC-1583544.

26. J. Hermann, R. A. DiStasio Jr., A. Tkatchenko, *Chem. Rev.*, 2017, **117**, 4714-4758.
27. A. Ambrosetti, N. Ferri, R. A. DiStasio Jr., A. Tkatchenko, *Science*, 2016, **351**, 1176.
28. G. Lu, R. Y. Liu, Y. Yang, C. Fang, D. S. Lambrecht, S. L. Buchwald, *J. Am. Chem. Soc.* 2017, **139**, 16548-16555.

1. B. P. Jacobs, P. T. Wolczanski, Q. Jiang, T. R. Cundari, S. N. MacMillan, *J. Am. Chem. Soc.*, 2017, **139**, 12145-12148.
2. D. J. Liptrot, J. D. Guo, S. Nagase, P. P. Power, *Angew. Chem. Int. Ed.*, 2016, **55**, 14766-14769.
3. D. J. Liptrot, P. P. Power, *Nature Rev. Chem.*, 2017, **1**, 0004 (1-12).
4. A. Casitas, J. A. Rees, R. Goddard, E. Bill, S. DeBeer, A. Fürstner, *Angew. Chem. Int. Ed.*, 2017, **56**, 10108-10113.
5. J. P. Wagner, P. R. Schreiner, *Angew. Chem. Int. Ed.* 2015, **54**, 12274-12296.
6. J. P. Wagner, P. R. Schreiner, *J. Chem. Theor. Comp.*, 2016, **12**, 231-237.
7. S. Rösel, H. Quanz, C. Logemann, J. Becker, E. Mossou, L. Cañadillas-Delgado, E. Caldeweyher, S. Grimme, P. R. Schreiner, *J. Am. Chem. Soc.* 2017, **139**, 7428-7431.
8. a) S. Grimme, J.-P. Djukic, *Inorg. Chem.*, 2010, **49**, 2911-2919; b) S. Grimme, J.-P. Djukic, *Inorg. Chem.*, 2011, **50**, 2619-2628.
9. a) C.-Y. Lin, J.-D. Guo, J. C. Fettinger, S. Nagase, F. Grandjean, G. J. Long, N. F. Chilton, P. P. Power, *Inorg. Chem.*, 2013, **52**, 13584-13593; b) C. L. Wagner, L. Tao, E. J. Thompson, T. A. Stich, J. Guo, J. C. Fettinger, L. A. Berben, R. D. Britt, S. Nagase, P. P. Power, *Angew. Chem. Int. Ed.* 2016, **55**, 10444-10447.
10. *Handbook of Bond Dissociation Energies in Organic Compounds*, Y.-R. Luo, Ed., CRC Press: New York, 2003.
11. J. L. Bennett, T. P. Vaid, P. T. Wolczanski, *Inorg. Chim. Acta*, 1998, **270**, 414-423.
12. H. E. Bryndza, L. K. Fong, R. A. Paciello, W. Tam, J. E. Bercaw, *J. Am. Chem. Soc.*, 1987, **109**, 1444-1456.
13. Y. Jiao, M. E. Evans, J. Morris, W. W. Brennessel, W. D. Jones, *J. Am. Chem. Soc.*, 2013, **135**, 6994-7004.
14. W. A. Herrmann, *Angew. Chem. Int. Ed. Engl.*, 1978, **17**, 800-812.
15. T. M. Trnka, R. H. Grubbs, *Acc. Chem. Res.*, 2001, **34**, 18-29.
16. M. Dartiguenave, M. J. Menu, E. Deydier, Y. Dartiguenave, H. Siebald, *Coord. Chem. Rev.*, 1998, **178**, 623-663.
17. N. D. Harrold, A. R. Corcos, G. L. Hillhouse, *J. Organomet. Chem.* 2016, **813**, 46-54.
18. a) D. F. Evans, *J. Chem. Soc.*, 1959, 2003-2005; b) E. M. Schubert, *J. Chem. Educ.*, 1992, **69**, 62.
19. H. H. Karsch, *Chem. Ber.*, 1977, **110**, 2222-2235.
20. H. H. Karsch, H.-F. Klein, H. Schmidbaur, *Chem. Ber.* 1977, **110**, 2200-2212.
21. B. K. Bower, H. G. Tennent, *J. Am. Chem. Soc.*, 1972, **94**, 2512-2514.
22. R. A. Lewis, B. E. Smiles, J. M. Darmon, S. C. E. Stieber, G. Wu, T. W. Hayton, *Inorg. Chem.*, 2013, **52**, 8218-8227.
23. E. K. Byrne, K. H. Theopold, *J. Am. Chem. Soc.*, 1989, **111**, 3887-3896.
24. P. T. Wolczanski, *Organometallics*, 2017, **36**, 622-631.
25. H. B. Abrahamson, K. L. Brandenburg, B. Lucero, M. E. Martin, *Organometallics*, 1984, **3**, 1379-1386.